Generation of multiple Bessel beams for a biophotonics workstation

T. Čižmár,[1*] V. Kollárová,[2] X. Tsampoula,[1] F. Gunn-Moore,[3] W. Sibbett,[1] Z. Bouchal,[2] and K. Dholakia[1]

[1]*School of Physics & Astronomy, University of St Andrews, North Haugh, St Andrews, Fife, KY16 9SS, Scotland*

[2]*Department of Optics, Palacky University, 17. Listopadu 50, 772 07 Olomouc, Czech Republic*

[3]*School of Biology, Bute Building, University of St Andrews, St Andrews, Fife, KY16 9TS, Scotland*

[*]*Corresponding author: tc51@st-andrews.ac.uk*

Abstract: We present a simple method using an axicon and spatial light modulator to create multiple parallel Bessel beams and precisely control their individual positions in three dimensions. This technique is tested as an alternative to classical holographic beam shaping commonly used now in optical tweezers. Various applications of precise control of multiple Bessel beams is demonstated within a single microscope giving rise to new methods for three-dimensional positional control of trapped particles or active sorting of micro-objects as well as "focus-free" photoporation of living cells. Overall this concept is termed a Biophotonics Workstation where users may readily trap, sort and porate material using Bessel light modes in a microscope.

OCIS codes: (000.0000) General.

References and links

1. J. Durnin, J. J. Miceli, and J. Eberly, "Diffraction-free beams," Phys. Rev. Lett. **58**, 1499–1501 (1987).
2. Z. Bouchal, J. Wagner, and M. Chlup, "Self-reconstruction of a distorted nondiffracting beam," Opt. Commun. **151**, 207–211 (1998).
3. V. Garcés-Chávez, D. Roskey, M. D. Summers, H. Melville, D. McGloin, E. M. Wright, and K. Dholakia, "Optical levitation in a Bessel light beam," Appl. Phys. Lett. **8**, 4001–4003 (2004).
4. L. Paterson, E. Papagiakoumou, G. Milne, V. Garcés-Cháves, T. Briscoe, W. Sibbett, L. Dholakia, and A. Riches, "Passive optical separation within a 'nondiffracting' light beam," Journal of Biomedical Optics **12**(054017) (2007).
5. T. Čižmár, V. Garcés-Chávez, K. Dholakia, and P. Zemánek, "Optical conveyor belt for delivery of submicron objects," Appl. Phys. Lett. **86**, 174,101–1–174,101–3 (2005).
6. T. Čižmár, V. Kollárová, Z. Bouchal, and P. Zemánek, "Sub-micron particle organization by self-imaging of non-diffracting beams," New. J. Phys. **8**, 43 (2006).
7. C. Sheppard and A. Choudhury, "Annular pupils, radial polarization, and superresolution," Applied Optics **43**(22), 4322 – 4327 (2004).
8. X. Tsampoula, V. Garcés-Cháves, M. Comrie, D. Stevenson, B. Agate, C. Brown, F. Gunn-Moore, and K. Dholakia, "Femtosecond cellular transfection using a nondiffracting light beam," Appl. Phys. Lett. **91**(5), 053,902 (2007).
9. S. Schmid, G. Thalhammer, K. Winkler, F. Lang, and J. Denschlag, "Long distance transport of ultracold atoms using a 1D optical lattice," New J. Phys. **8**, 159 (2006).
10. B. P. S. Ahluwalia, X.-C. Yuan, S. H. Tao, J. Bu, H. Wang, X. Peng, and H. B. Niu, "Microfabricated-composite-hologram-enabled multiple channel longitudinal optical guiding of microparticles in nondiffracting core of a Bessel beam array," Appl. Phys. Lett. **87**, 084,104 (2005).

11. Z. Jiang, Q. Lu, and Z. Liu, "Propagation of apertured Bessel beams," Applied Optics **34**(31), 7183 – 7185 (1995).
12. Z. Bouchal, "Controlled spatial shaping of nondiffracting patterns and arrays," Optics Letters **27**(16), 1376 – 1378 (2002).
13. Z. Bouchal, "Vortex array carried by a pseudo-nondiffracting beam," J. Opt. Soc. Am. A **21**(9), 1694 – 1702 (2004).
14. H. Little, C. Brown, V. Garcés-Chávez, W. Sibbett, and K. Dholakia, "Optical guiding of microscopic particles in femtosecond and continuous wave Bessel light beams," Optics Express **12**(11), 2560–2565 (2004).
15. J. W. Goodman, *Introduction to Fourier Optics* (McGraw-Hill, 1968).
16. J. Lin, X. Yuan, S. Tao, and R. Burge, "Collinear superposition of multiple helical beams generated by a single azimuthally modulated phase-only element," Optic letters **30**(24), 3266 – 3268 (2005).
17. J. E. Curtis, B. A. Koss, and D. G. Grier, "Dynamic holographic optical tweezers," Opt. Commun. **207**, 169–175 (2002).
18. V. Jarutis, R. Paškauskas, and A. Stabinis, "Focusing of Laguerre-Gaussian beams by axicon," Opt. Commun. **184 1-4**, 105–112 (2000).
19. O. Brzobohatý, T. Čižmár, and P. Zemánek, "High quality quasi-Bessel beam generated by oblate-tip axicon," Submitted to Optics Express (2008).
20. G. Milne, K. Dholakia, D. McGloin, K. Volke-Sepulveda, and P. Zemanek, "Transverse particle dynamics in a Bessel beam," Optics Express **15**(21), 13,972 – 13,987 (2007).
21. C. T. A. Brown, D. J. Stevenson, X. Tsampoula, C. McDougall, A. A. Lagatsky, W. Sibbett, F. J. Gunn-Moore, and K. Dholakia, "Enhanced operation of femtosecond lasers and applications in cell transfection," Journal of Biophotonics (2008).
22. D. Stevenson, B. Agate, X. Tsampoula, P. Fischer, C. T. A. Brown, W. Sibbett, A. Riches, F. Gunn-Moore, and K. Dholakia, "Femtosecond optical transfection of cells:viability and efficiency," Optics Express **14**(16), 7125–7133 (2006).
23. L. E. Barrett, J. Y. Sul, H. Takano, E. J. Van Bockstaele, P. G. Haydon, and J. H. Eberwine, "Region-directed phototransfection reveals the functional significance of a dendritically synthesized transcription factor," Nature Methods **3**(6), 455 – 460 (2006).

1. Introduction

Propagation-invariant optical fields, in particular Bessel beams (BBs), have been studied intensively and are finding an increasing frequency of application in many areas of science [1]. They belong to the group of "non-diffracting" beams whose lateral intensity profile remains unchanged during propagation in free space. In addition, they offer a number of interesting features such as the ability to reconstruct themselves after encountering an obstacle [2]. The ideal form of such a field would carry an infinite amount of energy, and therefore they cannot be experimentally realized in such an ideal form, but over a limited distance very good approximations known as quasi-Bessel beams may be generated.

The zero-order Bessel beam retains its high intensity central core along its propagation length whereas higher order BBs have a phase singularity (and therefore zero intensity) on the optical axis with a well quantified orbital angular momentum. In the area of optical micromanipulation BBs, have been used for various applications including long-distance guiding of colloids [3], passive sorting of particles and living cells [4] or generating large arrays of optical traps in counterpropagating or co-propagating BBs [5, 6]. Importantly, these light fields are expanding to other applications in interdisciplinary science such as microscopy [7], cell transfection [8] and atomic transport [9]. Diffractive optics and notably a conical glass element, the axicon, offer an excellent route to create single Bessel beams. Spatial light modulators (SLM) are powerful tools for dynamically reconfiguring the intensity profile of light fields in an arbritary fashion and may be used to generate BBs. To enhance their applicability it would be useful to generate arbitrary arrays of BBs in a three-dimensional space and be able to manoeuvre them at will within a sample chamber for both lateral and axial movement within a given volume.

Any attempt to achieve this directly behind an uniformly illuminated SLM would require compromising this original aim due to a number of limitations. An array of Bessel beams can be generated by splitting the SLM chip into a number of subdomains and providing an axicon-

phase modulation over each of them. A similar approach was demonstrated in [10] using an axicon array diffractive element. It is also possible to produce several parallel Bessel beams with the same propagation distance displaced in three dimensions by using annular subdomains with the same thickness (circular subdomain as the special case), but the feasibility of full 3D positioning the beams is strongly limited whilst avoiding overlapping of each of the subdomains, that would otherwise bring significant aberrations. A major drawback of this solution is that for axially displaced BBs the power is not distributed equally. Generally there is no flexibility in power distribution between the resulting beams and the power in each beam can only be reduced by lowering the diffraction efficiency of the modulation. In addition to the power and efficiency problems, the quality of the beams is poor due to the limited size of each subdomain [11] and the interference with light coming from unused parts of the SLM thereby resulting in strong oscillations of the on-axis intensity.

In this work we explore a different approach towards achieving this goal and in particular to exploit the spectral modulation of BBs, which, as we shall describe, is a more powerful generic concept than standard holographic beam shaping in this instance. This concept was originally described by Bouchal[12, 13], where the phase modulation is applied on the annular spatial spectrum field (far-field) of a BB and can result in the splitting of the original BB into a number of parallel BBs where the position of each of them can be precisely and independently controlled. Control and modification of a spatial spectrum of axicon-generated Bessel beam (AGBB) provides a highly efficient and versatile approach to the generation of several BBs in one given experiment. At the same time it offers the possibility of spatial filtration that permits the removal of undesired parts of spectrum originating from axicon imperfections or the arbitrary manipulation of the topological charge (order) of the BB.

We demonstrate a variety of applications of these beams notably those where the use of a focused Gaussian beam is limiting. BBs are particularly suitable for long distance guiding [14]. With the possibility of axial positioning one can transport selected particles between separate planes in a sample thus providing a new method of active sorting. The prospect of splitting the BBs into multiple lateral arrays and shifting them axially enables 3-D position control of trapped microparticles. Finally, the "focus-free" transfection of living cell using ultrashort pulse BBs is presented where the precise positioning of the maximal intensity region on the cell membrane is no longer the prerequisite associated with a Gaussian beam. Overall this embodies the concept of Biophotonics Workstation where the user may now use such Bessel modes to trap, sort and porate cellular material at will.

2. Theoretical background

2.1. Spatial spectrum modulation

In this section we explain how the modulation of spatial spectrum in the afocal plane inside a magnifying telescope influences the output field. The mathematics presented is for monochromatic light within a scalar paraxial approach, where we considered ideal thin lenses and unimportant phase constants have been neglected. Let us define an initial field $A(x,y)$ in a front focal plane of the first telescope lens L_1 with focal length of f_1 (see Fig. 1).

The spatial spectral field $S(u,v)$ arising in the back focal plane of L_1 is a Fourier transform of field $A(x,y)$ in frequencies $(u/\lambda f_1, v/\lambda f_1)$, where λ is wavelength of the used light [15].

$$S(u,v) = \iint_{-\infty}^{\infty} \frac{A(x,y)}{i\lambda f_1} e^{\frac{-2\pi i}{\lambda f_1}(xu+yv)} \mathrm{d}x\mathrm{d}y. \tag{1}$$

In the back focal plane of the second lens L_2 we obtain a field $B_0(\bar{x},\bar{y})$ as the reconstructed

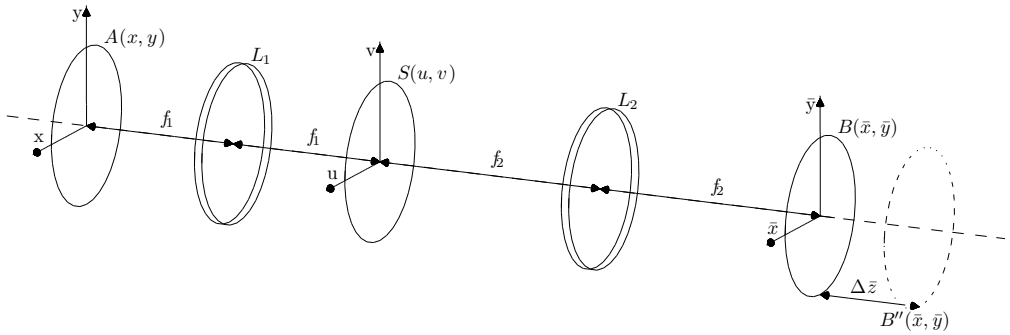

Fig. 1. 4f system consisted of two lenses L_1 and L_2 in afocal assembly. f_1 and f_2 are focal lengths of lenses L_1 and L_2 respectively, $A(x,y)$ is the object field in the back focal plane of the lens L_1, $S(u,v)$ is the spatial spectrum of $A(x,y)$ generated by the lens L_1 and $B(\bar{x},\bar{y})$ is the magnified image of $A(x,y)$.

image of field $A(x,y)$:

$$B(\bar{x},\bar{y}) = \iint_{-\infty}^{\infty} \frac{S(u,v)}{i\lambda f_2} e^{\frac{-2\pi i}{\lambda f_2}(u\bar{x}+v\bar{y})} \mathrm{d}u\mathrm{d}v. \tag{2}$$

Combination of (1) and (2) leads to a relation between $A(x,y)$ and $B(\bar{x},\bar{y})$ in the form:

$$B(\bar{x},\bar{y}) = \frac{f_1}{f_2} A\left(-\frac{f_1}{f_2}\bar{x}, -\frac{f_1}{f_2}\bar{y}\right), \tag{3}$$

that highlights the well-known properties of a magnifying telescope.

Since the spatial spectrum modulation is provided in practice by an optical component such as a transparent wedge, lens, grating or hologram it can be generally described as a multiplication of the spectrum $S(u,v)$ by an arbitrary complex function $f(u,v)$ such as

$$0 \leq |f| \leq 1 \tag{4}$$

for every u and v. A linear phase modulation can be linked to the translational property of a Fourier transform such that:

$$\begin{aligned} S_l(u,v) &= S(u,v) \cdot e^{\frac{2\pi i}{\lambda f_2}(\Delta\bar{x}u+\Delta\bar{y}v)} \\ &\equiv S(u,v) \cdot f_l(\Delta\bar{x},\Delta\bar{y}) \end{aligned} \tag{5}$$

where $\Delta\bar{x}$ and $\Delta\bar{y}$ are arbitrary parameters and it leads to a lateral shift in the position of the original image:

$$B_l(\bar{x},\bar{y}) = \frac{f_1}{f_2} A\left[-\frac{f_1}{f_2}(\bar{x}-\Delta\bar{x}), -\frac{f_1}{f_2}(\bar{y}-\Delta\bar{y})\right]. \tag{6}$$

Similarly, it can be shown that applying a quadratic phase:

$$\begin{aligned} S_q(u,v) &= S(u,v) \cdot e^{\frac{-\pi i\Delta\bar{z}}{\lambda f_2^2}(u^2+v^2)} \\ &\equiv S(u,v) \cdot f_q(\Delta\bar{z}) \end{aligned} \tag{7}$$

leads to a longitudinal shift of the image plane to the distance of $\Delta\bar{z}$ as demonstrated on the Fig. 1. Since both of the modulations (6) and (8) can be easily combined we can apply them efficiently to control the position of reconstructed image in three dimensions:

$$S_{3D}(u,v) = S(u,v) \cdot f_l(\Delta\bar{x},\Delta\bar{y})\ f_q(\Delta\bar{z}). \tag{8}$$

Generation of arbitrary positioned multiple images can be provided by superposition of individual modulations (8):

$$S_{mult}(u,v) = S(u,v) \cdot \frac{1}{n} \sum_{j=1}^{n} f_l^j(\Delta\bar{x},\Delta\bar{y})\ f_q^j(\Delta\bar{z}), \tag{9}$$

where the term $1/n$ needs to be inserted to fulfill the condition (4). Therefore, the transparency of an optical component representing this modulation is on average $1/n$ and each individual image carries a $1/n^2$ fraction of the total power. A more general form of (9) involves the arbitrary distribution of the total power between the generated images:

$$S_{mult}(u,v) = S(u,v) \cdot \frac{1}{\sum_{j=1}^{n} c_j} \sum_{j=1}^{n} c_j f_l^j(\Delta\bar{x},\Delta\bar{y})\ f_q^j(\Delta\bar{z}), \tag{10}$$

where $\left(c_n / \sum_{j=1}^{n} c_n \right)^2$ gives the fraction of the total power carried by j-th beam. A better balance can be provided by omitting the amplitude modulation and using only phase modulation for (9) but this has the drawback of producing other unwanted 'ghost' images. The general analysis of this influence is beyond the scope of this paper but, for example, by creating two laterally displaced images using a binary phase mask with step phase lift equal to π gives in average around 40% of the input power for each image and 20% of the power is wasted in the ghost images. For specific cases there might be better approaches how to transfer a complex modulation to a phase only modulation [16].

2.2. *Axicon generated Bessel beam*

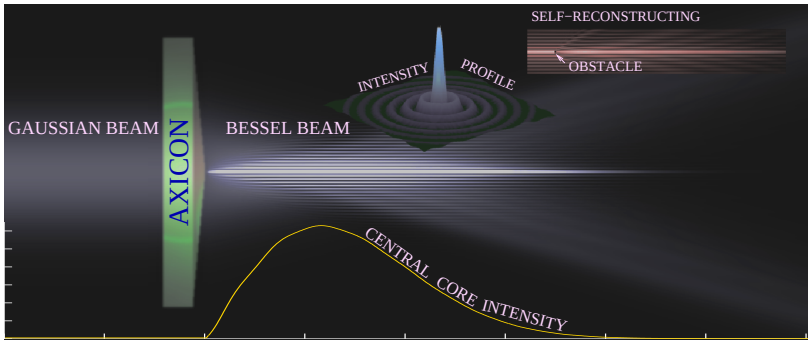

Fig. 2. Numerically evaluated axicon generated Bessel beam. The insets shows lateral intensity cross-section, on-axis intensity and the demonstration of self-reconstructing property of Bessel beams

In the context of the previous explanation, the concept of holographic beam shaping for optical tweezers can be understood as the case where a large Gaussian beam approximating a

plane wave is used as a spatial spectrum [17]. However, the theory introduced above is valid for any optical field and in this section we present the possibility of using an axicon generated Bessel beam (AGBB) as the object for spatial spectrum modulation.

Generally non-diffracting beams are special solutions of the wave equation such that their intensity profile remains unchanged during propagation. One of the most commonly used representations is the zero-order Bessel beam:

$$E_{BB}(\rho, z) = E_{ax} J_0(k\rho \sin(\alpha_0)) e^{ikz\cos(\alpha_0)}, \tag{11}$$

where ρ and z are the cylindrical coordinates ($\rho = \sqrt{x^2 + y^2}$), E_{ax} and α_0 are arbitrary parameters. The AGBB is a spatially limited approximation of the ideal zero-order Bessel beam and it is generated by a Gaussian beam passing through a conical lens (axicon). Figure 2 illustrates such a beam. Based on the approximate analytical solution by Jarutis et al. [18] the on-axis intensity is given by:

$$I(\rho = 0, z) = I_0 \frac{2\pi kz}{\cos(\alpha_0)} \sin(\alpha_0)^2 \, e^{-2\left(\frac{z\tan(\alpha_0)}{w}\right)^2}, \tag{12}$$

where I_0 is the on-axis intensity of the incident Gaussian beam, w is the waist size of the Gaussian beam and α_0 is related to the apex angle of the axicon τ by:

$$\alpha_0 = \frac{n_a - n_s}{n_s} \frac{\pi - \tau}{2}, \tag{13}$$

where n_a is the refractive index of the axicon and n_s is the refractive index of the surrounding medium. The spatial spectrum of AGBB has a ring-like (annular))shape with a ring thickness proportional to $1/w$ (see Fig. 3) giving an off-axis delta function for $w \to \infty$. For quantification

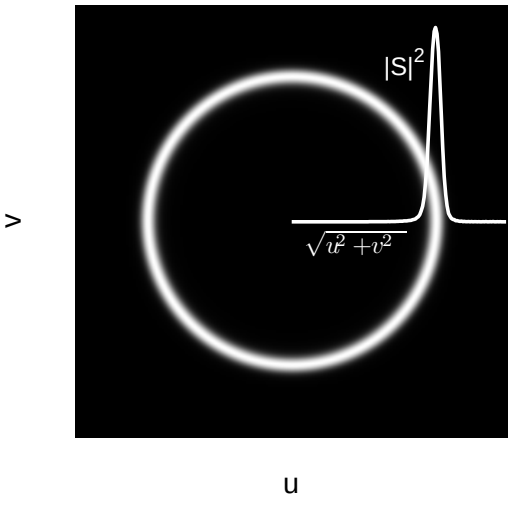

Fig. 3. A typical spatial spectrum of an AGBB.

of the axial range of AGBB existence is traditionally used a quantity $z_{max} = \frac{w}{\tan(\alpha_0)}$ that comes from the geometrical conformation of the field behind an axicon and it is the distance where the beam intensity is larger than 0.323 of its maximal value. Figure 4 shows various spatial spectrum modulations applied to an AGBB resulting in the possibility of 3-D positioning of the image as well as the generation of multiple images.

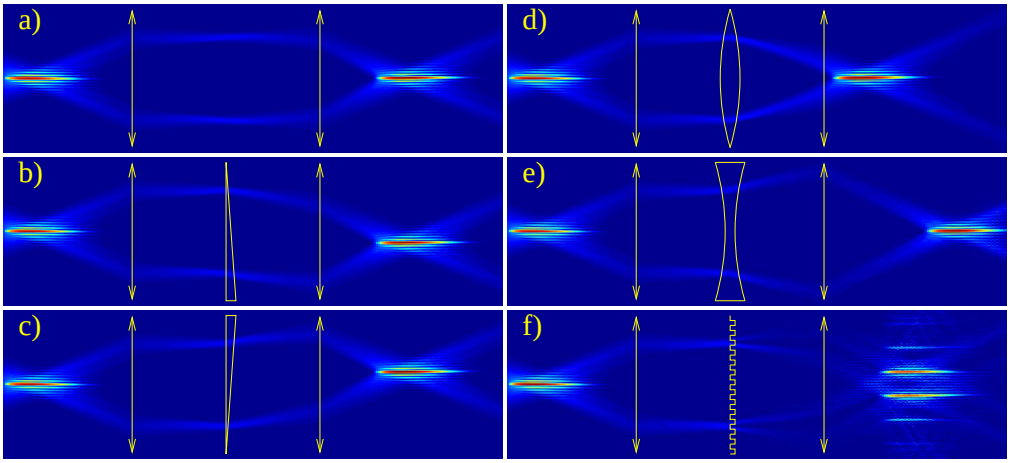

Fig. 4. A numerical simulation of the spatial spectrum modulation of an AGBB by a) empty, b, and c) linear, d, and e) quadratic phase functions and f) binary phase masks.

Using an AGBB also brings several other possibilities for spatial spectrum modulation. As shown by [18] the spatial spectrum of zero-order Bessel beams and higher-order Bessel beams differs only in helical phase term $e^{in\psi}$ where n is the topological order of Bessel beam and ψ is the azimuthal coordinate of the spatial spectrum ($\psi = \tan^{-1}(v/u)$). Therefore, using this (phase only) term for spatial spectrum modulation brings the possibility of generating any-higher order Bessel beam easily from the original zero-order Bessel beam thus providing control over the resulting angular momentum of the image field. In the case of generating multiple images (9), we can change the order in each individual image independently as shown in Fig. 5a.

The other option for the case of AGBBs is the possibility of spatial filtering. As shown by Brzobohaty et al. [19] commercially available axicons typically bring several aberrations due to the imperfect, oblate tip that results in periodic modulation of the on-axis intensity and low-pass filtering of unwanted parts of spectra leads to a restoration of the high quality Bessel beam with a smooth on-axis profile. Even a phase-only modulation can be used to filter out the unwanted parts of spectra in combination with the linear phase. In other words, a linear phase is applied only at the desired parts of spectra leading to the generation of filtered laterally-shifted Bessel beams as demonstrated in Fig. 5b. Because the thickness of a ring-like spatial spectrum of

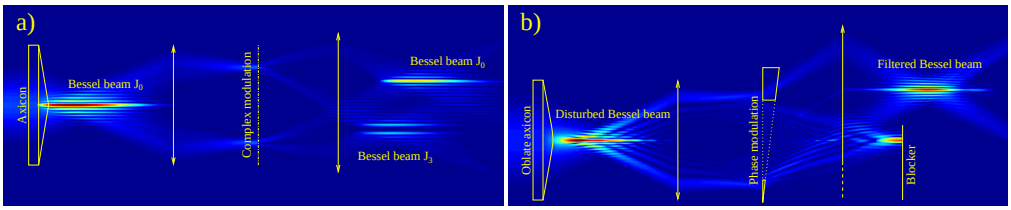

Fig. 5. a) A demonstration of the generation of higher-order Bessel beams using complex modulation. This example shows two axially and laterally displaced Bessel beams of orders 0 and 3. If the amplitude modulation is removed and phase-only modulation is used, the power in each beam is higher, but several ghost orders appear. b) A demonstration of spatial filtration of a Bessel beam generated by an imperfect axicon having an oblate tip.

AGBB is proportional to $1/w$ and therefore to $1/z_{max}$ as well, spatial spectrum filtration can be applied as in the above case to reduce the size of the spectral ring thickness thus increasing the

distance of Bessel beam propagation, but the penalty is significant power loss.

3. Experimental realization

3.1. Experimental setup

To verify the principles discused here, we developed an experimental setup using a phase only spatial light modulator (SLM) (also called programmable phase modulator) to control the spatial spectrum of an AGBB (see Fig. 6). Tthe SLM is a computer driven device designed to

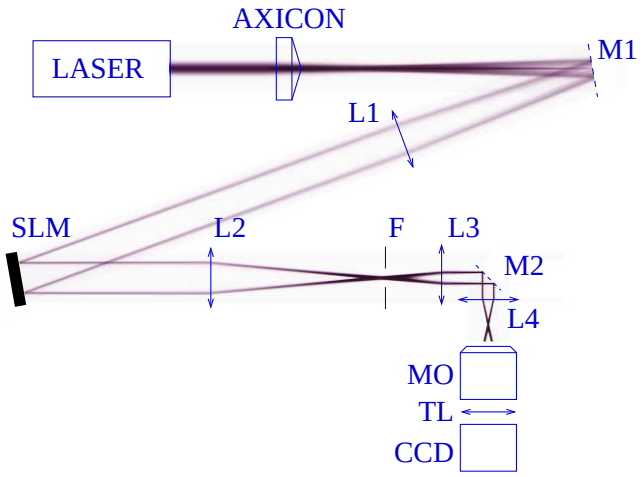

Fig. 6. The experimental setup: M1 and M2 - mirrors, L1-L4 - lenses, SLM - spatial light modulator, MO - microscope objective, TL - tube lens, CCD - CCD camera

provide and dynamically reconfigure any phase modulation along its active area.

As a laser source we used Ti:Sapphire laser (Coherent MIRA 900) at $\lambda_{vac} = 790$ nm with a total power of 800 mW that could be deployed in CW or pulsed (modelocked) regime (200 fs pulses with 76 MHz repetition rate). The output laser beam had a Gaussian profile of waist size $w = 530$ µm. Using an axicon with $\tau = 178.6°$ we generated an AGBB with parameters of $\alpha_0 = 0.35°$ and $z_{max} = 89$ mm. Based on the observed axial modulation of its on-axis intensity we concluded that the axicon tip was slightly oblate and that spatial filtration should be applied to ensure a high quality in the generated beam. The modulation of the spatial spectrum was provided on the SLM (Hamamatsu X8267-13) in the afocal plane of a telescope comprising lenses L1 and L2 with focal lengths of $f_1 = 1000$ mm and $f_2 = 400$ mm respectively. The focal length of L1 was selected so that the spatial spectrum ring of the AGBB (with the radius of 6.1 mm) could be as large as possible to fit into the area of SLM and thus assure the finest possible modulation. Even though the diffraction efficiency of the SLM was high there is always some power left in the zero diffraction order as well as in other unwanted orders coming from orthogonal lay-out of the SLM matrix. These orders were removed by filter F having a circular aperture in the back focal plane of lens L2. In the case of the spatial filtration, this filter also blocks the beam containing the unwanted parts of spectra (where no modulation is applied) because it appears in the area of zero order. To ensure a suitable size and sufficient power for optical micromanipulation, the beam was further demagnified on the second telescope that comprised lenses L3 and L4 with focal lengths of $f_3 = 150$ mm and $f_4 = 8$ mm giving a final AGBB with $\alpha_0 = 16.4°$ and $z_{max} = 40$ µm. The back focal plane of L4 was imaged by a microscope objective (Mitutoyo M Plan Apo 80x) and a 200 mm tube lens onto a CCD (BASLER piA640-210gm).

To find the optimal parameters for spatial filtration we selected the largest annular area (with radius 6.1 mm and thickness 1.7 mm) that overlapped the spatial spectrum ring on the SLM when all of the axial modulation of the resulting AGBB was removed. This brought a slight increase in the axial extent of the AGBB from its original 40 μm length to about 55 μm. The unique benefit of the spatial filtration method is a saving of a significant amount of computation time : about 5$\times$ less time is necessary to calculate the phase function on the annular area compared to evaluating the function for the whole SLM chip. The area imaged on the CCD corresponds to 120×90 μm^2 and applying the linear phase modulation to position the AGBB image across the whole CCD chip gives the total efficiency of the whole system between 55-70% depending on the diffraction efficiency for each modulation used. The setup is noticeably similar to an arrangement used for holographic optical tweezers. Solely replacing the axicon in our geometry with a lens means one can easily switch between these geometries.

3.2. Controlling software

For controlling the SLM we developed a mouse-driven interface using LabView that enables all the principles demonstrated in the previous sections to be demonstrated. When clicking on the camera image downloaded into the interface, the program calculates the phase modulation and applies it on the SLM via second output from a graphics card so the center of single or multiple AGBBs appears in the position of mouse. Revolving the mouse wheel controls the quadratic phase on SLM thereby resulting in axial positioning of the beam.

The software also includes a correction for the angle of incidence of the original beam, control of separation and orientation of multiple beams (for 2 and 3 beams at the current version) and also the possibility to add a helical phase modulation that switches between different orders of the AGBB (see video 1 - real-time record showing the full functionality of the system).

4. Applications

For all of the applications described here, we inserted a sample chamber consisting of a microscope slide or a petri dish, spacer, microobjects dispersed in water medium and cover-glass into the setup at the position of back focal plane of lens L4. Because the resulting AGBBs are propagating in water, their lateral cross-section remains the same, but the distance of their propagation is increased to ≈ 75 μm.

4.1. Active sorting of microobjects

The optical forces of an AGBB acting on high index dielectric spherical particles have been reported in [20] and their detailed explanation is beyond the scope of this paper. For particles smaller or comparable with the size of the AGBB central core the forces are attracting the particle into the central core laterally and pushing the particle axially in the direction of the AGBB propagation. Therefore, by positioning the AGBB on the selected particle we can transfer the particle into a remote plane. This can be applied efficiently for the active sorting of microobjects where all the selected particles can be expelled one-by-one from the bottom plane where all the particles are located due to the sedimentation. Figure 7 and video 2 shows this when applied to a solution of 2 μm and 5 μm polystyrene particles where the smaller ones are separated from the bottom to top of the sample chamber.

4.2. 3-D positioning of microobjects

Three-dimensional trapping of an object in a single BB is not possible due to the minimal intensity gradient along its axis, but it can be achieved in a geometry of 2 counterpropagating beams. Using our setup it can be done by creating 2 axially displaced beams and reflecting the

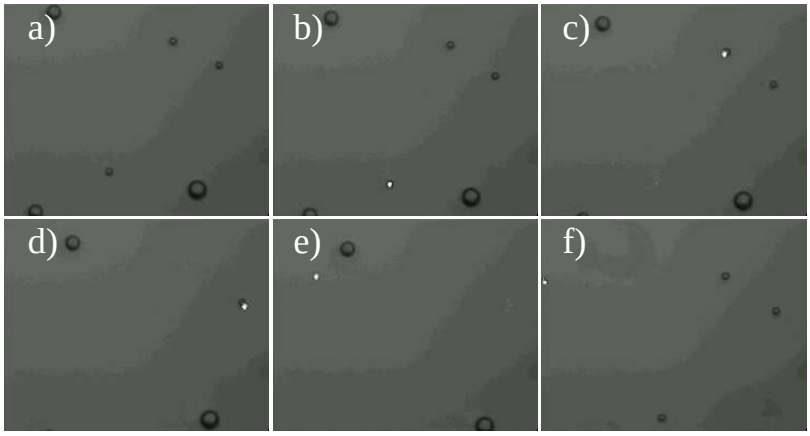

Fig. 7. Active sorting of 2 µm and 5 µm polystyrene particles: a) - initial layout of particles at the bottom plane of the sample chamber; b)-e) - one by one transport of 2 µm particles; f) - top plane of the sample chamber showing sorted 2 µm particles.

furthest one backwards using dielectric mirror that replaces the microscope slide. Given that both beams are coherent, this would cause an interference of the beams resulting of standing wave field distribution. This geometry, known as an optical conveyor belt [5], was used for the delivery of objects over very large areas (by altering the phase in one of the BBs) and can be provided by offsetting the phase modulation for one of the generated beam on the SLM. For some particle sizes, however, the standing wave trapping is not possible and the particles will move freely in the z direction. To overcome this, a time-shared generation of these two beams can be used thus removing the interference structure and even-though the axial intensity envelope is changing slowly we can always find for any required position of the trap in the chamber space an optimal axial displacement of the beams to get the strongest axial trapping. This is demonstrated on 3 µm polystyrene particles shown in video 3. The maximal rate of switching between the beams is 12 Hz for the SLM used.

4.3. Optical transfection of living cells

The ability to introduce at will foreign DNA or therapeutic agents inside the living mammalian cell for purposes of gene therapy, disease diagnosis and treatment, without compromising the cell viability, is one of the most challenging and exciting tasks in the life sciences. This technique, known as transfection, has been revolutionized by the development of state of state-of-the-art femtosecond lasers, making optical transfection a non-invasive and ultra-precise alternative to conventional disruptive and often toxic transfection techniques [21]. Femtosecond cellular transfection is a two-photon process, with the two-photon excitation occurring only within the small focal region [22]. This imposes strict requirements for precise positioning the laser focus on the cell membrane, when optical transfection is performed using a tightly focused Gaussian beam. Problems associated with critical alignment, when moving from cell to cell, can be circumvented by using BBs. Due to its non-diffracting nature, a Bessel beam acts as a rod of light, maintaining a long axial range over which successful transfection can occur [8]. Our present study involves femtosecond optical transfection of Chinese hamster ovary (CHO) cells using an SLM-controlled AGBB, as shown in Fig. 6. The CHO monolayer was washed twice with OPTI-MEM, according to our previously described protocol [8] and was subsequently exposed to 30 µl of OPTIMEM solution containing 3 µg of mitoDSRed plasmid which encodes a mitochondrially targeted discoideum red fluorescent protein (BD Biosciences,

Oxford, UK). A type-0 thickness glass coverslip (BDH, Poole UK) was floated on top of the solution to prevent the sample from drying out. Each cell in the sample dish was treated with three laser exposures, each of 40 msec duration, at a power level of 30 mW in the central core. 48 hours after laser treatment, the cells were observed under a microscope for red fluorescent protein (RFP) expression and successful photoporation was achieved. Bessel beam transfection shows transfection efficiences comparbel to the Gaussian beam [8].

5. Conclusions

The spatial spectrum modulation of an axicon-generated Bessel beam is a simple way to multiplex and control this beam for biophotonics applications. The supporting theory shows that spatial spectrum modulation can be applied regardless of which object field is used and for a combination of linear and quadratic phase modulations it always leads to 3-D positioning of the image field. Generation of multiple images is discussed together with the influence of phase-only modulation. For the case of an AGBB, we also described the possibility of orbital angular momentum control and spatial filtration to improve the quality of the resulting AGBB. Implementing all these possibilties, we developed a device that offers full Bessel beam control for many studies in optical trapping, sorting and cell transfection. We showed that even though the axial intensity gradient of the AGBBs is small and cannot be used for 3-D trapping in a single beam, it is large enough to provide stable 3-D confinement of particle in a geometry that involves time-shared counter-propagating beams. Finally, we described applications for active sorting of micro-objects and photoporation of living cells where the use of an AGBB is preferable to its Gaussian beam counterpart.

The ability of making multiple parallel Bessel Beams at will for photoporation studies has major advantages for the field of Cell Biology. Here we describe not only the ability to produce a 'user friendly' device but also the ability to target many cells at the same time with additionally the unique ability of selectively choosing a cell or group of cells within a large population of cells. Furthermore it also provides an improved method for providing the ability to target different sub-cellular targets, the importance of which has been shown in the transfection of polarised cells such as hippocampal neurons [23].

6. Acknowledgments

We thank the UK Engeneering and Physical Sciences Rresearch Council for funding. This work was partially supported by the Research projects Measurement and Information in optics MSM 6198959213, Center of Modern Optics LC06007 and project FT-TA2/059 of the Czech Ministry of Industry and Trade.